Study of the Effects of D_2O Circulation

N. S. Oblath and A. W. P. Poon
Lawrence Berkeley National Laboratory, Berkeley, CA 94720

September 12, 2000

Abstract

The Sudbury Neutrino Observatory (SNO) has been collecting data since November 1999. The study of whether or not the D_2O circulation affects the data is an important part of understanding how the SNO detector behaves. This report looks at several characteristics of the data to determine to what extent the D_2O circulation affects the data. We found that there is no evidence for any dependence of event rates in the cleaned data sets on the state of D_2O circulation.

1 Introduction

Before the SNO physics data can be reliably analyzed, the systematics of the detector must be adequately understood. The effects of the D_2O circulation on the behavior of the detector needs to be investigated.

In this study, we have analyzed runs between December 1999 and April 2000. Runs in November were not included in the analysis because during that month the water contained higher levels of contaminants. We have analyzed only events in Sets A and B as generated by the data splitter in SNOMAN. The runs included in this analysis are listed in Tables 1 and 2, according to whether the D_2O circulation was on or off during the run. Runs for which the D_2O circulation was on for only part of the run were excluded. The runs listed in these tables are the ones recommended by the SNO Run Selection Committee for solar neutrino analysis up to mid-April 2000.

To determine whether the D_2O circulation affects the SNO data, we have compared various distributions for runs with the circulation on and off. The comparisons were made using data that had been cleaned by the WCA FiST filters as well as the SNOMAN DAMN cuts (mask=0xF16FE5). All one dimensional spectra presented in this report are normalized to the total run time (taking the data splitting into account). Using time normalized runs allowed the comparison not only of the shapes of the distributions, but also of the event rates.

Table 1: Runs with the D_2O circulation on.

10554	10650	10701	10704	10708
10734	10737	10741	10743	10776
10782	10805	10883	10943	10962
10969	10970	11347	11366	11383
11390	11417			

1.1 Run Time Calculations

We used data sets A and B generated by the data splitter in SNOMAN. Since we only looked at a subset of the data, we had to calculate the run times in this subset instead of doing a simple Δt subtraction between the run start and stop times. To determine the approximate run times for only data sets A and B, a histogram of the event times with bin widths of 30 seconds was made for each run. The live time for Sets A and B was then deduced from counting the non-empty time bins in these histograms.

Table 2: Runs with the D_2O circulation off.

10534	10536	10549	10551	10555	10638	10649	10651	10655	10675
10677	10678	10680	10686	10687	10700	10705	10706	10709	10710
10714	10735	10736	10738	10739	10740	10742	10744	10747	10748
10749	10756	10762	10770	10773	10775	10779	10781	10783	10784
10797	10801	10803	10804	10806	10811	10813	10815	10821	10826
10828	10836	10840	10841	10843	10869	10871	10873	10876	10878
10879	10881	10882	10884	10885	10886	10887	10891	10894	10922
10923	10924	10925	10927	10932	10933	10935	10936	10938	10939
10942	10944	10948	10949	10950	10951	10953	10954	10955	10956
10959	10961	10963	10972	10975	10976	11269	11271	11272	11281
11286	11289	11291	11303	11310	11312	11313	11368	11371	11377
11381	11384	11389	11393	11397	11399	11400	11402	11406	11407
11415	11429	11431	11433	11436	11437	11443	11444	11446	11462
11466	11474	11479	11481	11489	11490	11493	11498	11502	11504
11506	11508	11510	11512	11525	11528	11531	11532	11533	11537
11539	11541	11543	11544	11549	11550				

Since our analysis of the event rate during D_2O circulation depends on the calculated run times, it is important to be sure that they were calculated correctly. Using 30-second bins gave us run times with fairly high resolution. To make sure that no large errors were made, we calculated a rough estimate of the run times by calculating $\frac{2}{3}(t_{stop} - t_{start})$ for each run, and compared that to the values determined by the method described above. Table 3 includes the run times calculated by both methods, and their percentage difference. The difference is insignificant for our study.

2 Analysis

2.1 Nhits

We analyzed the runs listed in Tables 1 and 2. Figures 1 and 2 show the Nhits spectra for the FiST and DAMN filtered data, respectively. In these plots the spectra for the D_2O circulation-on and off runs are superimposed. Two features are clear in these plots. First, the DAMN data and the FiST data have very similar Nhits distributions. The histograms match very closely. The second feature visible in the Nhits plots is that at low Nhits (<40 Nhits), the event rate in the circulation-on sample is higher than that in the circulation-off

Table 3: The total run times for data sets A and and B, of runs for which the D_2O circulation was on and for which it was off. Method 1 used histograms with 30-second bin widths to total the run times for each run. Method 2 used the following formula to determine the run time for each run: $\frac{2}{3}(t_{stop} - t_{start})$

D_2O Circ. State	Method 1 Time (sec)	Method 2 Time (sec)	Percent Error
on	267960	265745	0.8%
off	5257020	5382179	2.4%

sample. At higher Nhits (>60 Nhits), the circulation-on and the circulation-off event rates are consistent with each other, although the statistics are poor in the former.

When we inspected the data more closely, we realized that there is a strong sampling bias in the results presented in Figures 1 and 2. Most of the D_2O circulation-on runs listed in Table 1 were taken during the early phase of production running (late 1999), whereas most of the circulation-off runs are in 2000. We know from the data that the radioactivity in both the light and the heavy water are improving as production running progresses. Therefore, there is a strong sampling bias towards runs with higher low energy background in Figures 1 and 2 for the D_2O circulation-on runs. The fact that the biggest discrepancy between the circulation-on and off runs occurs at low Nhits supports this hypothesis.

To determine whether the aforementioned sampling bias is the cause of the difference between the circulation-on and off Nhits distributions, we compared the Nhits distribution for each circulation-on run to two circulation-off runs that were closest in time. We selected only those runs that were recommended by the Run Selection Committee (Table 2). Also, one of the two selected circulation-off runs must precede, while the other must follow the circulation-on run.

In Figure 3 we show the FiST filtered Nhits distribution for Run 10554, which is a D_2O circulation-on run. In the same figure, Nhits distributions from Run 10551 and 10555 are superimposed. It is clear that the Nhits distributions from these three runs are consistent with each other in the Nhits$\leq$40 region.

We performed this analysis on all of the D_2O circulation-on runs up to Run 10970 listed in Table 1. In Figure 4, the accumulative Nhits distributions for these circulation-on runs are shown. Also shown in the figure is the accumulative Nhits distributions for the two D_2O circulation-off runs closest to the circulation-on run. Unlike Figure 3 we have summed the circulation-off runs before and after the circulation-on run into one histogram. It is clear that at low Nhits, the discrepancy between circulation-on and off runs no longer exists. This statement holds for both FiST and DAMN reduced data sets. In Figure 5 the fractional

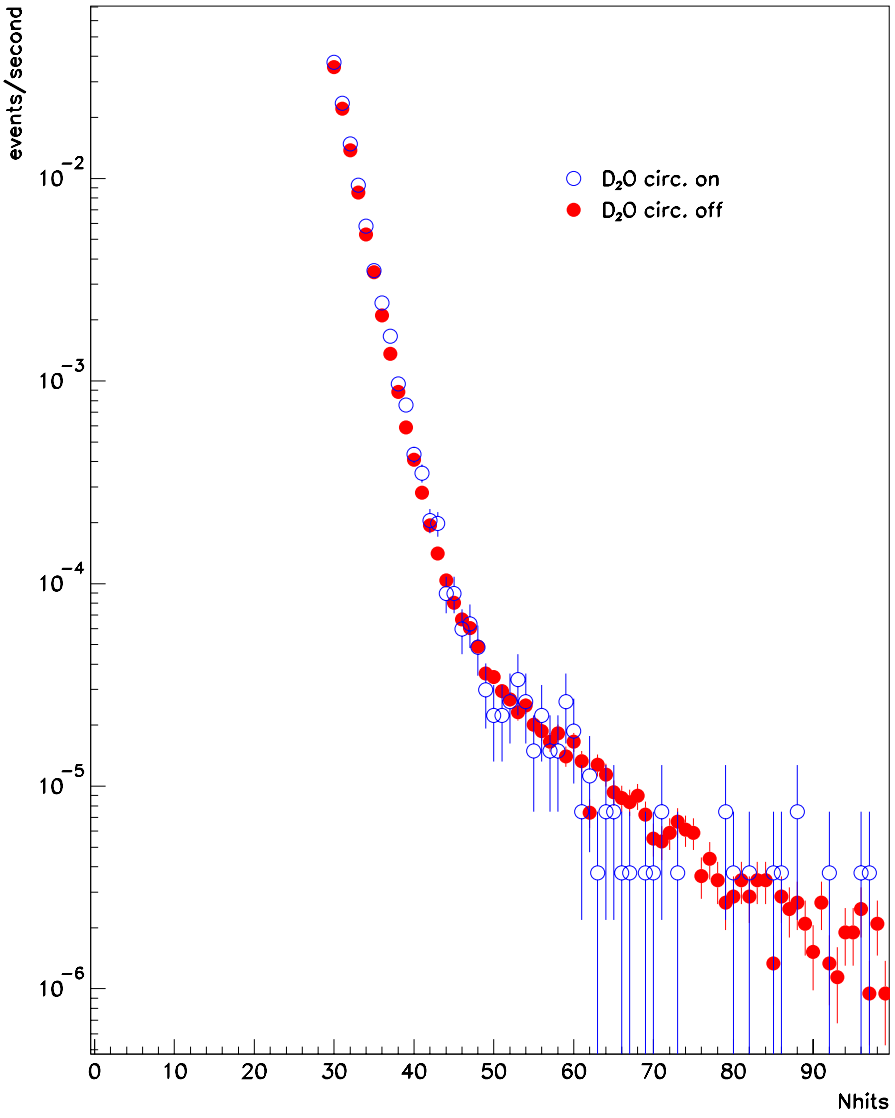

Figure 1: The Nhits spectra for runs with the D_2O circulation on and off, from the FiST filtered data set.

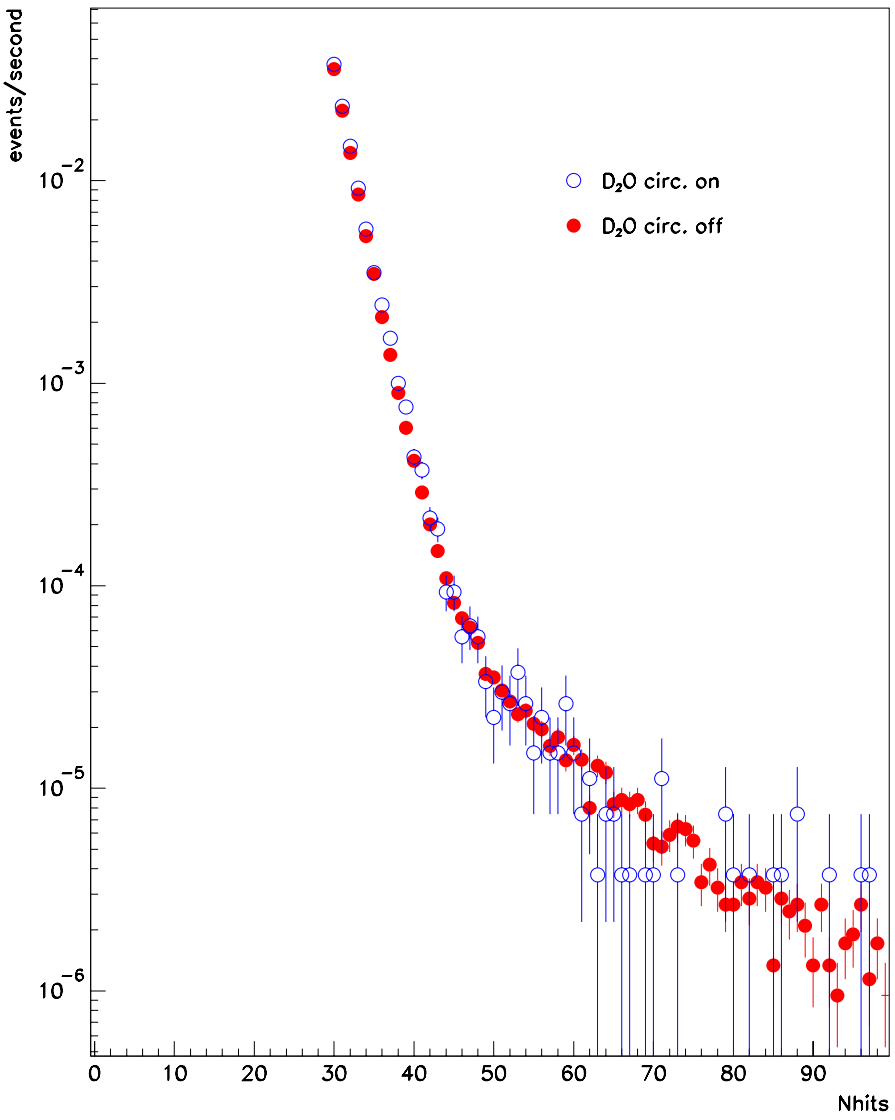

Figure 2: The Nhits spectra for runs with the D_2O circulation on and off, from the DAMN filtered data set.

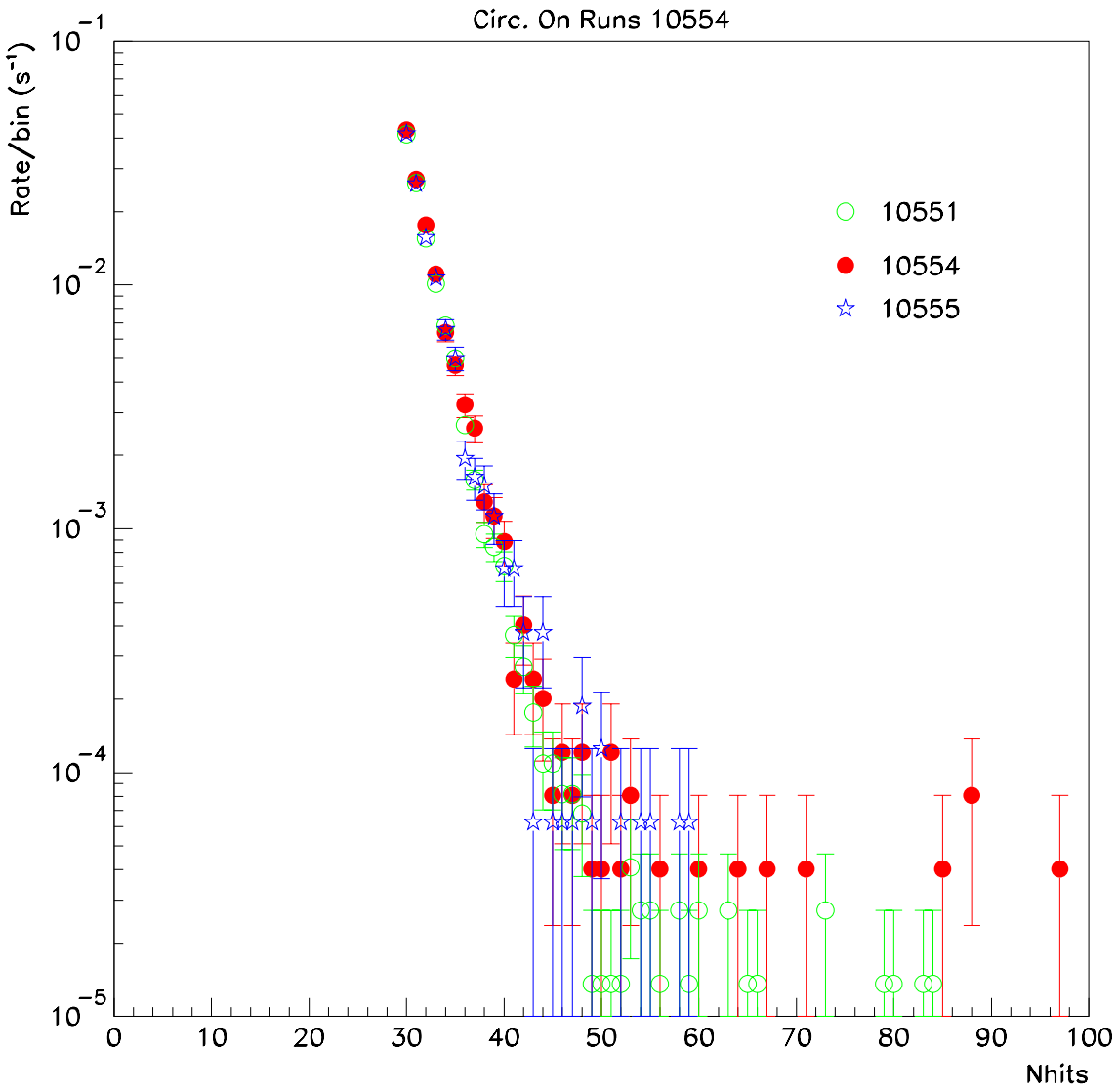

Figure 3: Nhits distribution for D_2O circulation-on Run 10554. Also shown are the Nhits distributions for the two circulation-off runs — Runs 10551 and 10555. The Nhits spectra for these three runs are consistent with each other in the Nhits$\leq$40 region.

difference between the Nhits spectra in Figure 4 is shown. We should point out that because most of the D_2O circulation-on runs are much longer in run time than the circulation-off runs, there must be more recorded events in the neutrino energy window in the circulation-off runs. Therefore, it appears that the event rate at Nhits$\geq$50 is higher for D_2O circulation-off runs.

2.2 Spatial Distribution

An analysis was conducted to investigate the spatial distribution of the events for the D_2O circulation-on and off samples. The event vertices were reconstructed with the elastic fitter, seeded with the grid fitter reconstructed vertex. Figures 6 and 7 show the R^3_{fit} distributions for the FiST and DAMN filtered data sets (Nhits$\geq$30) respectively. The shape of the plots is due to the increased levels of Uranium and Thorium in the acrylic sphere, light water and PSUP. The decays of those radioactive contaminants result in an increased number of events that are reconstructed to larger radial distance.

Again the event rates with the circulation-on runs are much higher than those seen with the circulation off. This is due to the sampling bias mentioned above. The shapes of the circulation-on and circulation-off curves are very similar, which further supports the sampling bias hypothesis. In order to minimize the sampling bias, we performed a similar sampling of circulation-off runs as mentioned above. Figure 8 shows the R^3_{fit} distributions for D_2O circulation-on Run 10554, and those for D_2O circulation-off Runs 10551 and 10555. There is no statistically significant difference between these three R^3_{fit} distributions.

The $cos\theta$ vs. ϕ plots allowed us to determine if the D_2O circulation caused any bias in distribution of the fit vertex locations. Here ($cos\theta$,ϕ) are the angular coordinates of the reconstructed vertex. For both the circulation-on and off runs, this analysis was done in three parts. The first was to look at all of the events for which a vertex was successfully found to be within the PSUP. The second step was to impose a 6 meter fiducial volume cut to focus on the events that were fitted to within the heavy water. The last step looked at those events with vertices that were fitted to within the light water. This is done for both the FiST and DAMN filtered data. Figures 9 and 10 show the $cos\theta$ vs. ϕ distributions for all of the events that were reconstructed to within the PSUP. These are density plots in which the size of the boxes in the plots represent the point density at the corresponding grid points.

An interesting feature that can be seen in each of the $cos\theta$ vs. ϕ plots is the cluster of events at the approximate coordinates $cos\theta = 0.75$, $\phi = 0.4$. This cluster exists regardless of whether the D_2O circulation is on and off. When using different fiducial volume cuts, we found that the majority of the events in this cluster are reconstructed near the acrylic vessel, although there is a tail into the D_2O volume. We will come back to this point later.

The locations of the water sample points were compared with these plots to see if there was any clustering of event vertices around them. Table 4 lists the ($cos\theta$,ϕ) coordinates of

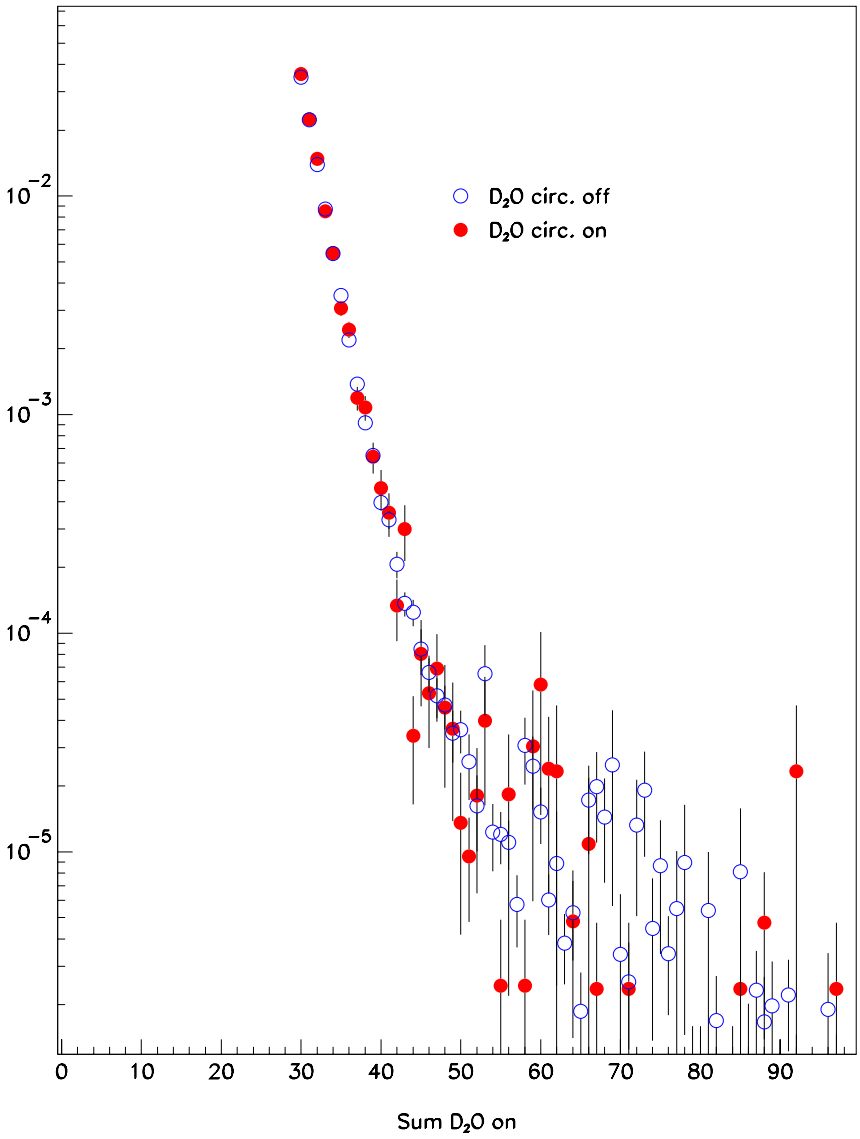

Figure 4: Accumulative Nhits distribution for DAMN reduced data in D_2O circulation-on runs up to Run 10970. Also shown are the accumulative Nhits distributions for the circulation-off runs closest in time to the circulation-on runs. The Nhits spectra for these two populations are consistent with each other in the Nhits$\leq$40 region.

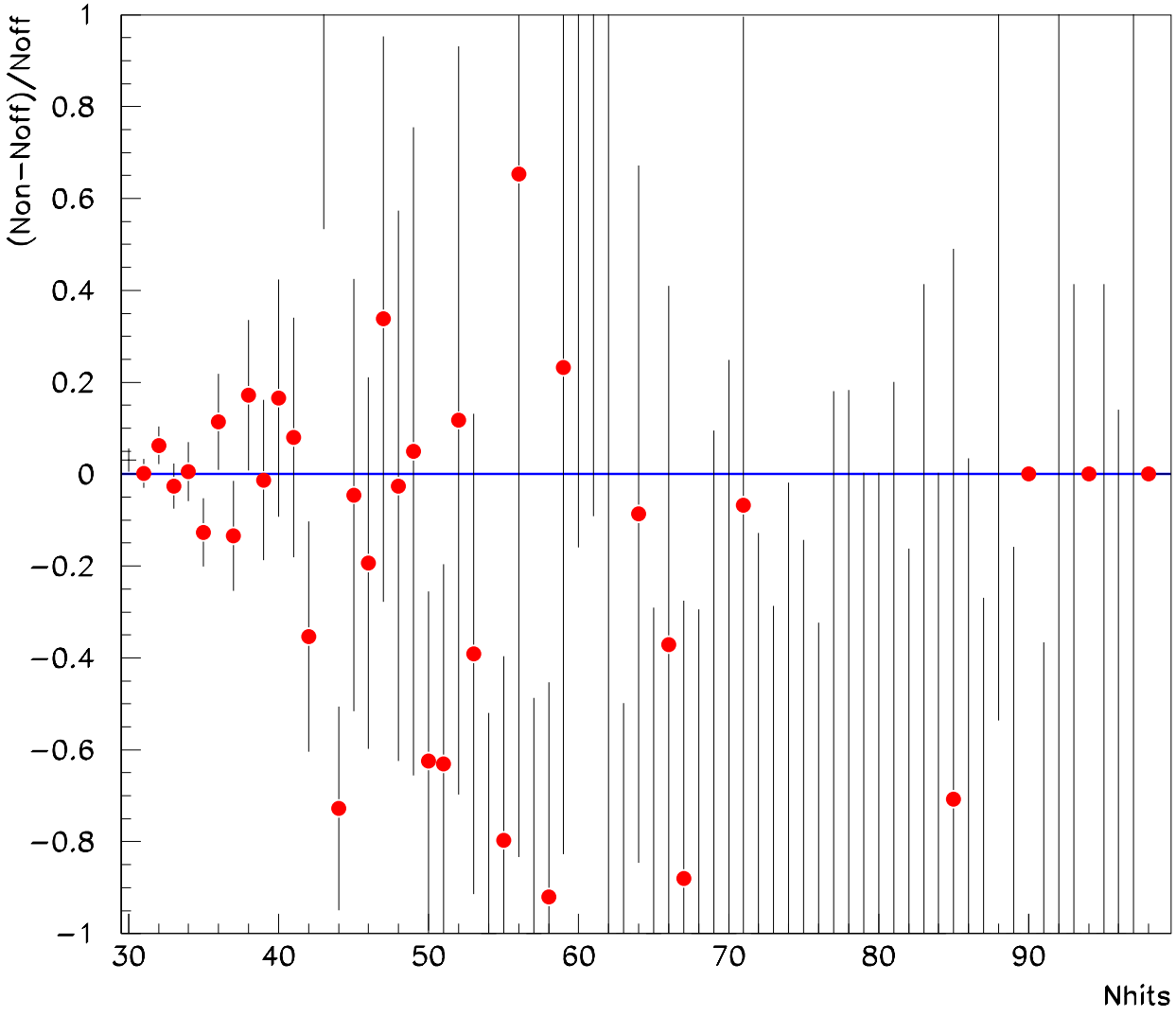

Figure 5: Fractional difference for D_2O circulation-on and circulation-off runs up to Run 10970. This figure shows the fractional difference between the Nhits spectra in Figure 4.

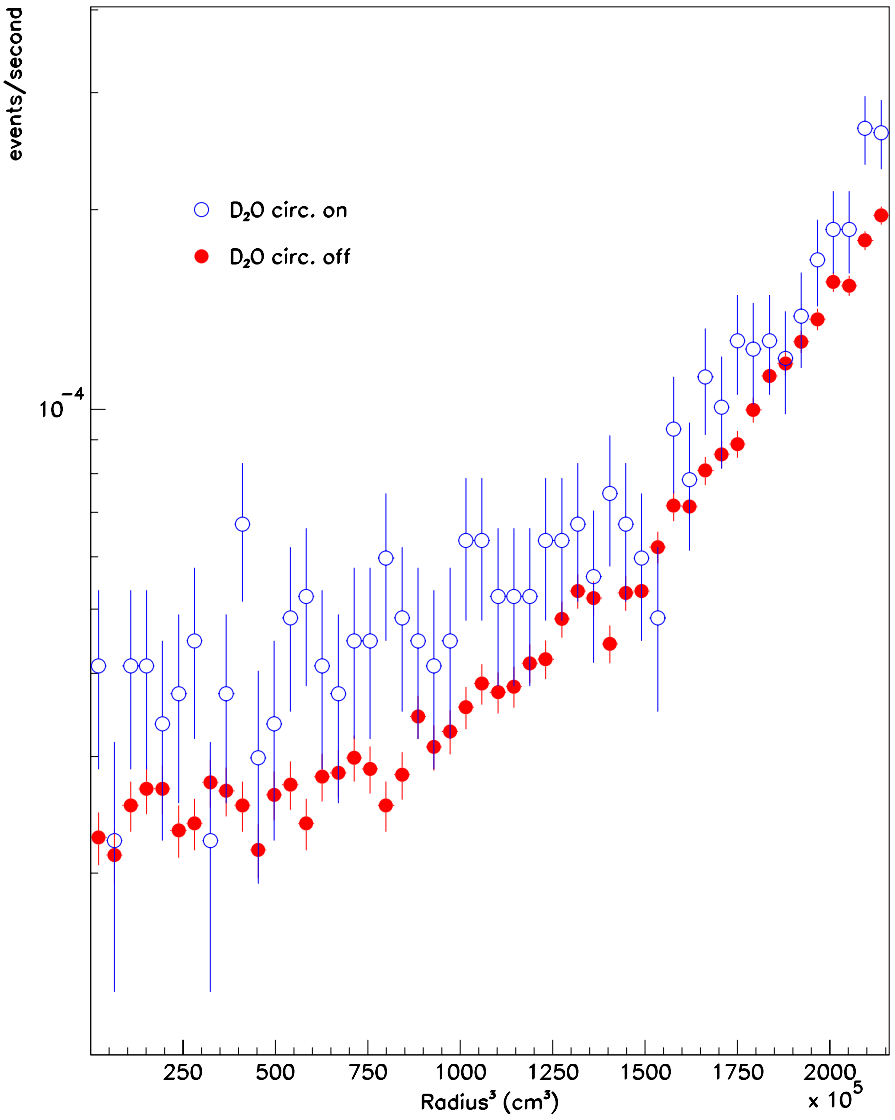

Figure 6: The R^3_{fit} for runs with the D_2O circulation on and off, from the FiST filtered data set.

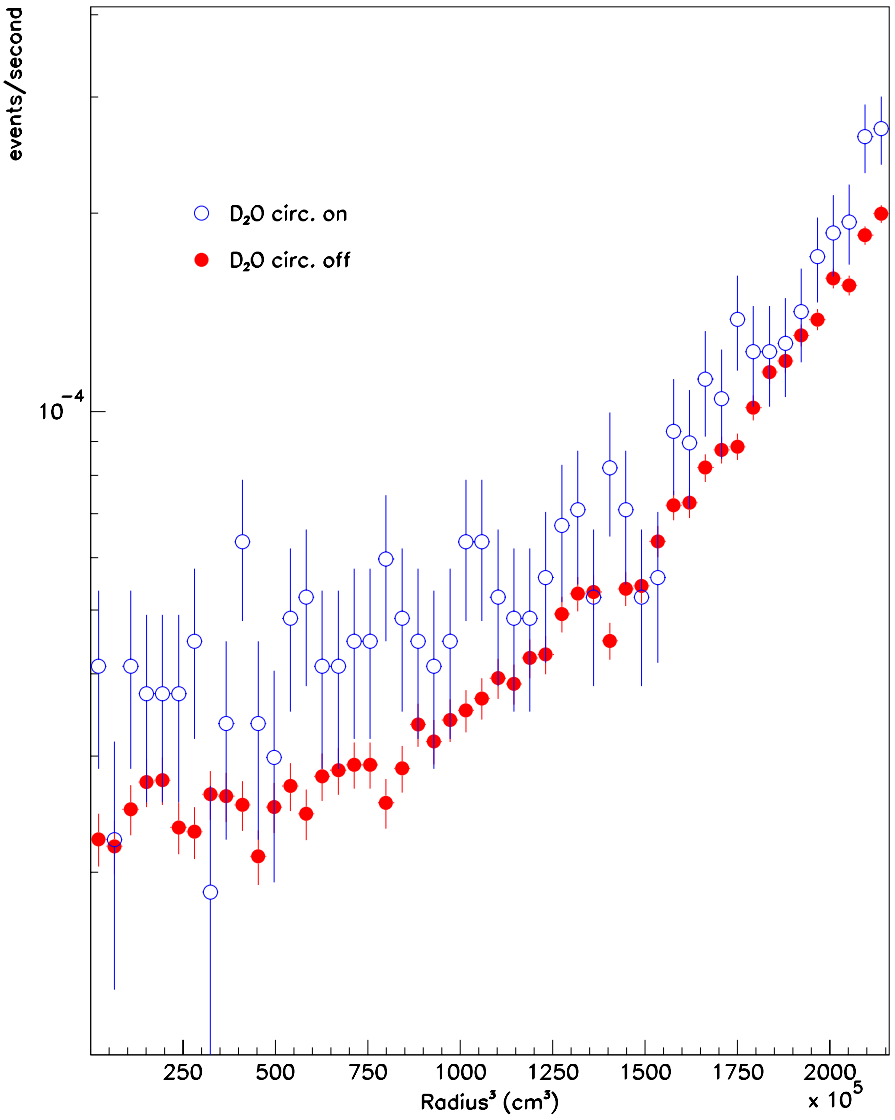

Figure 7: The R^3_{fit} for runs with the D_2O circulation on and off, from the DAMN filtered data set.

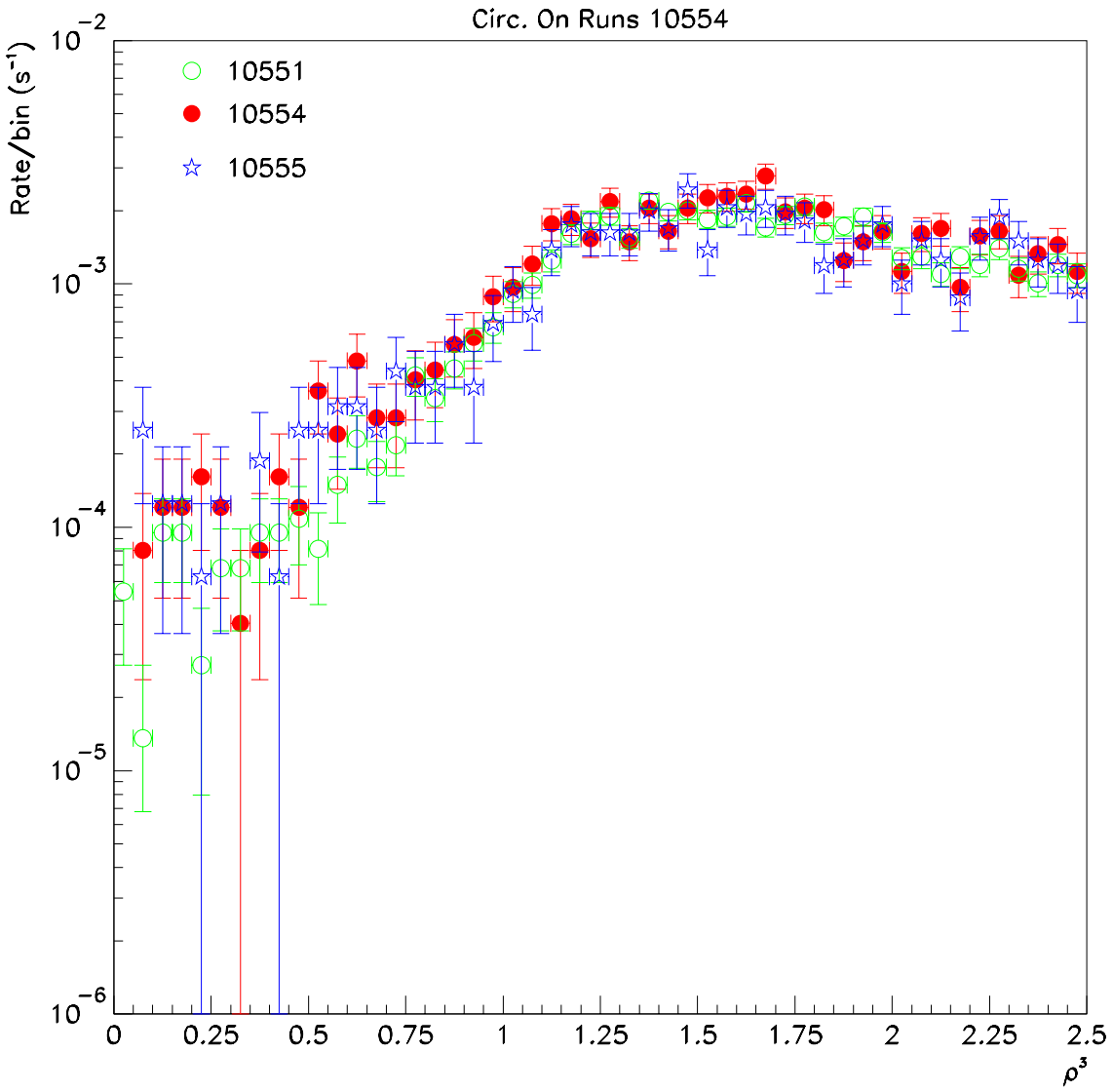

Figure 8: The R^3_{fit} for DAMN reduced data in D_2O circulation-on Run 10554. Also shown are the R^3_{fit} distributions for D_2O circulation-off Runs 10551 and 10555. In this plot, the plotted quantity ρ^3 is equivalent to $(R_{fit}/600\text{cm})^3$.

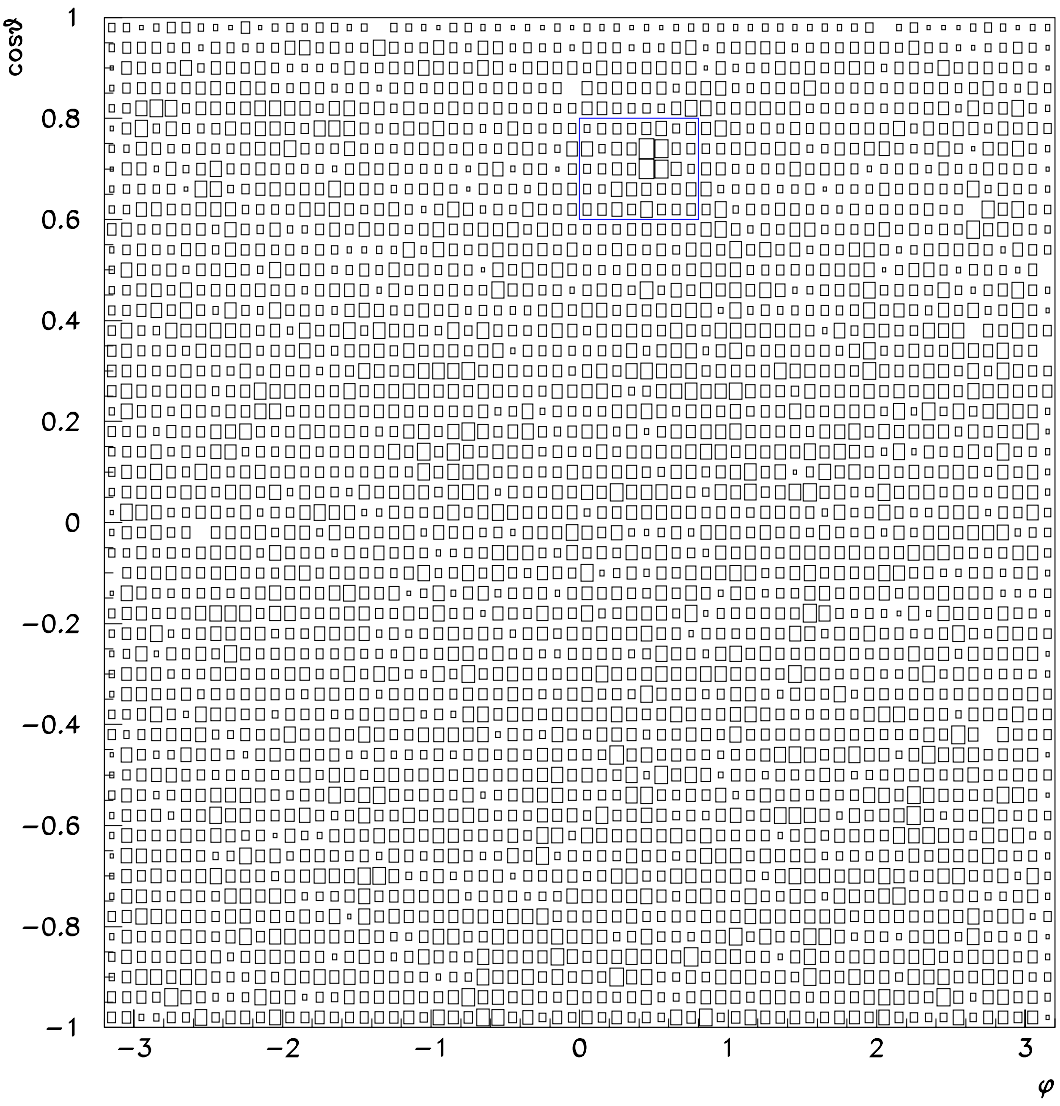

Figure 9: The $cos\theta$ vs. ϕ plot for runs with the D_2O circulation on, and from the DAMN filtered data set. Only events with Nhits$\geq$30 and reconstructed to within the PSUP are shown. This is a density plot in which the size of the boxes represent the point density at each grid point.

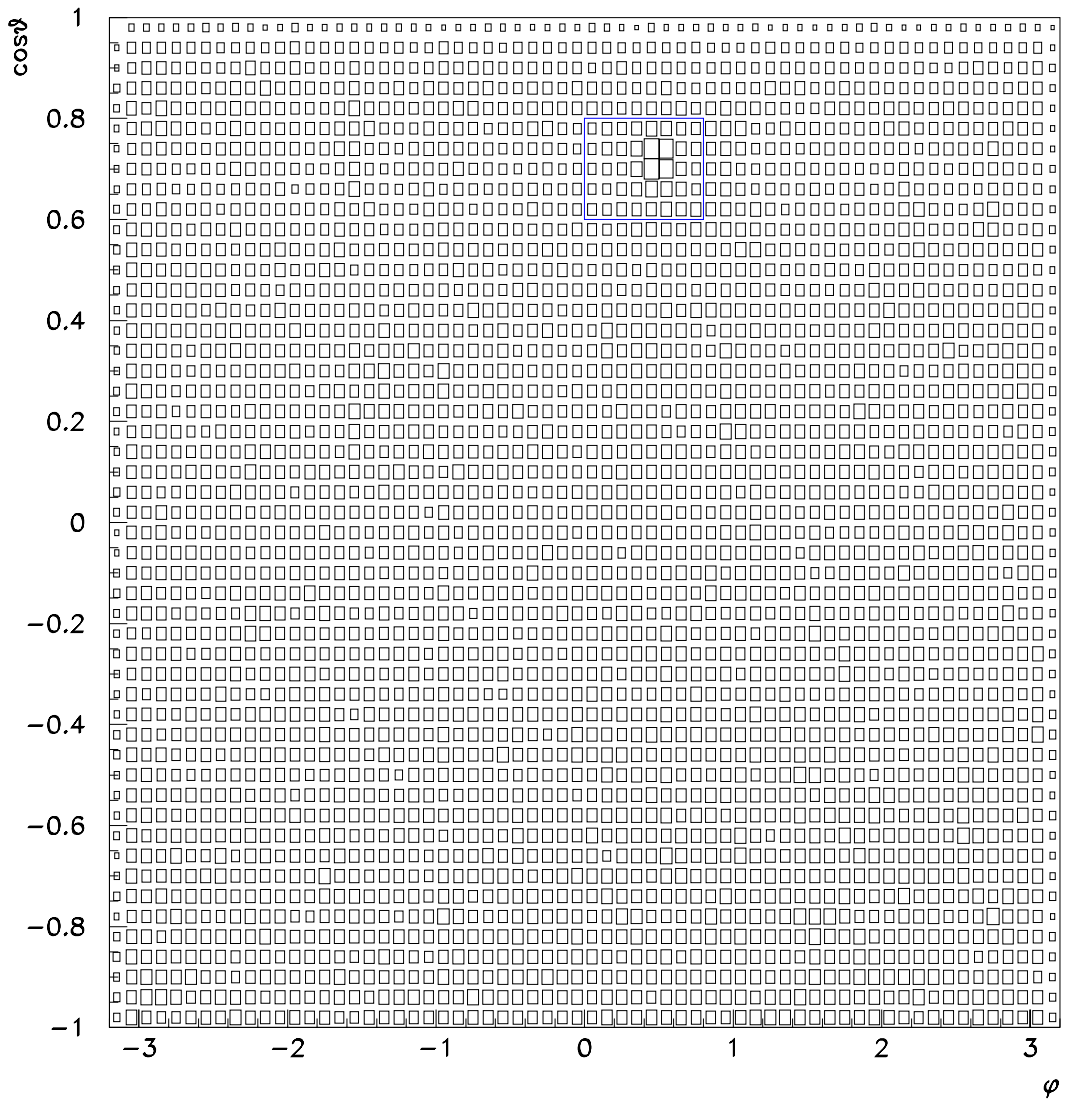

Figure 10: The $cos\theta$ vs. ϕ plot for runs with the D_2O circulation off, and from the DAMN filtered data set. Only events with Nhits$\geq$30 and reconstructed to within the PSUP are shown. This is a density plot in which the size of the boxes represent the point density at each grid point.

the sample points. There is no evidence of any such clustering around the D_2O sampling points in the heavy water plots or around the H_2O sampling pointss in the light water plots. The ($cos\theta$,ϕ) distribution does not appear to have any significant dependence on the D_2O circulation.

Table 4: D_2O and H_2O Sample Points[1]. Pipe Termination IDs 12 and 13 are outside of the PSUP and were therefore not part of this analysis.

Pipe Termination ID	Sample Point	$cos\theta$	ϕ
1	D_2O Return	0.993	-1.101
2	D_2O Supply Lower Hemisphere	1.000	-1.571
3	D_2O Sample Chimney	0.998	1.101
4	D_2O Sample Upper Hemisphere	0.993	1.101
5	D_2O Sample Upper Hemisphere	0.573	1.448
6	D_2O Sample Lower Hemisphere	-0.307	1.450
7	D_2O Sample Lower Hemisphere	-0.930	-1.534
8A	H_2O Feed	-0.160	1.487
8B	H_2O Feed	-0.160	1.487
9	H_2O Sample	-0.182	-0.277
10	H_2O Sample	-0.010	0.351
11	H_2O Sample	-0.168	0.314
14	H_2O Inner PSUP Fill Line	-1.000	—

Though it has no particular relation to the D_2O circulation, we investigated the mysterious clustering in Figures 9 and 10. When we visually scanned the events that lie within the window of $cos\theta \in [0.69, 0.80]$ AND $\phi \in [0.30, 0.72]$, we found that most of the events are either the so-called "Queen's events" with most PMT hits near the top of the detector, or events with fairly isotropic hit distribution in PSUP space. There was no particular run or group of runs from which these events originated.

The events in the cluster were compared with three other sample cuts, obtained by

rotating the original cut window around the detector in intervals of $\pi/2$ in ϕ. Table 5 quantitatively demonstrates two points. The event rates with the circulation on are the same, within errors, as the event rates with the circulation off. Each sample cut outside the "cluster box" is within statistical errors of the other two sample cuts.

Table 5: The event rates in the cluster cut window and in the three other sample cut windows for the D_2O circulation-on and circulation-off runs.

Cut Window	Circulation On Event Rate (events/second)	Circulation Off Event Rate (events/second)
Original Cut $cos\theta \in [0.69, 0.80]$ AND $\phi \in [0.30, 0.72]$	$(5.11 \pm 0.44) \times 10^{-4}$	$(4.98 \pm 0.10) \times 10^{-4}$
Sample Cut 1 $cos\theta \in [0.69, 0.80]$ AND $\phi \in [1.87, 2.29]$	$(3.06 \pm 0.34) \times 10^{-4}$	$(2.94 \pm 0.07) \times 10^{-4}$
Sample Cut 2 $cos\theta \in [0.69, 0.80]$ AND $\phi \in [-1.27, -0.85]$	$(3.47 \pm 0.36) \times 10^{-4}$	$(2.96 \pm 0.07) \times 10^{-4}$
Sample Cut 3 $cos\theta \in [0.69, 0.80]$ AND $\phi \in [-2.84, -2.42]$	$(3.09 \pm 0.40) \times 10^{-4}$	$(3.32 \pm 0.08) \times 10^{-4}$

There was a major repair done on the acrylic vessel during its construction. The location of this major repair is (65±9)° east of north, and (36.0±0.7)° from vertical[2]. This corresponds to $\cos\theta \in [0.80, 0.82]$ and $\phi \in [0.28, 0.59]$. This range of ($\cos\theta$, ϕ) is outside the cluster shown in Figures 9 and 10. What is interesting is that the ϕ coordinate of the cluster corresponds to those of the major repair very well, but with a slight offset in $\cos\theta$.

We looked at the clustered events further. We compared the events enclosed by a cut window with $\cos\theta \in [0.6, 0.8]$ and $\phi \in [0, 0.8]$ to events enclosed by cut windows of exactly the same size at random locations in the ($\cos\theta$, ϕ) plane. The former cut window is shown as the boxes in Figures 9 and 10. Nhits, R^3_{fit} $u.r$, and θ_{ij} distributions between the events in the cluster cut box and those in the random box were compared. These are shown in Figures 11, 12, 13, and 14. In particular, the solid histograms in these plots are the distributions in the cluster cut window, and the dashed histograms are the difference in distributions between those events in the cluster cut window and the random box. An Nhits≥30 cut, and a Rfit<650cm cut (where applicable) were used. From these figures, it appears that the cluster of events have an energy spectrum very similar to U and Th $\beta - \gamma$. And that these events are concentrated near the AV and are mostly directed outwards. We are investigating the origin of this clustering. We want to verify or nullify the hypothesis that whether this clustering of events is related to the major repair on the acrylic vessel.

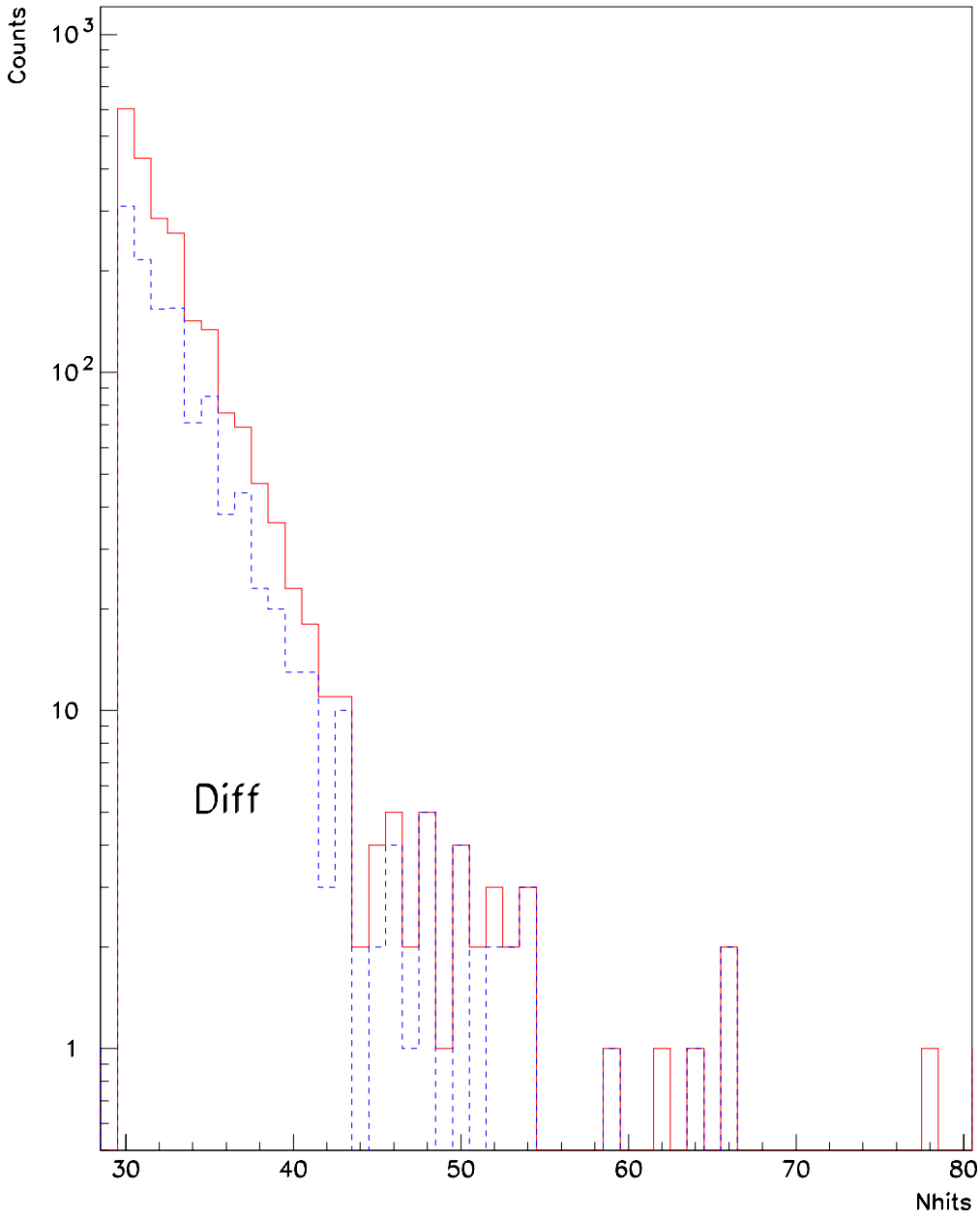

Figure 11: The Nhits distributions of those events in the cluster cut window are compared to those in a random cut window of the same size in the ($\cos\theta$,ϕ) space. The solid histogram is the Nhits distribution of the events in the cluster cut window. And the dashed histogram is the difference between this last distribution and that for a random cut window.

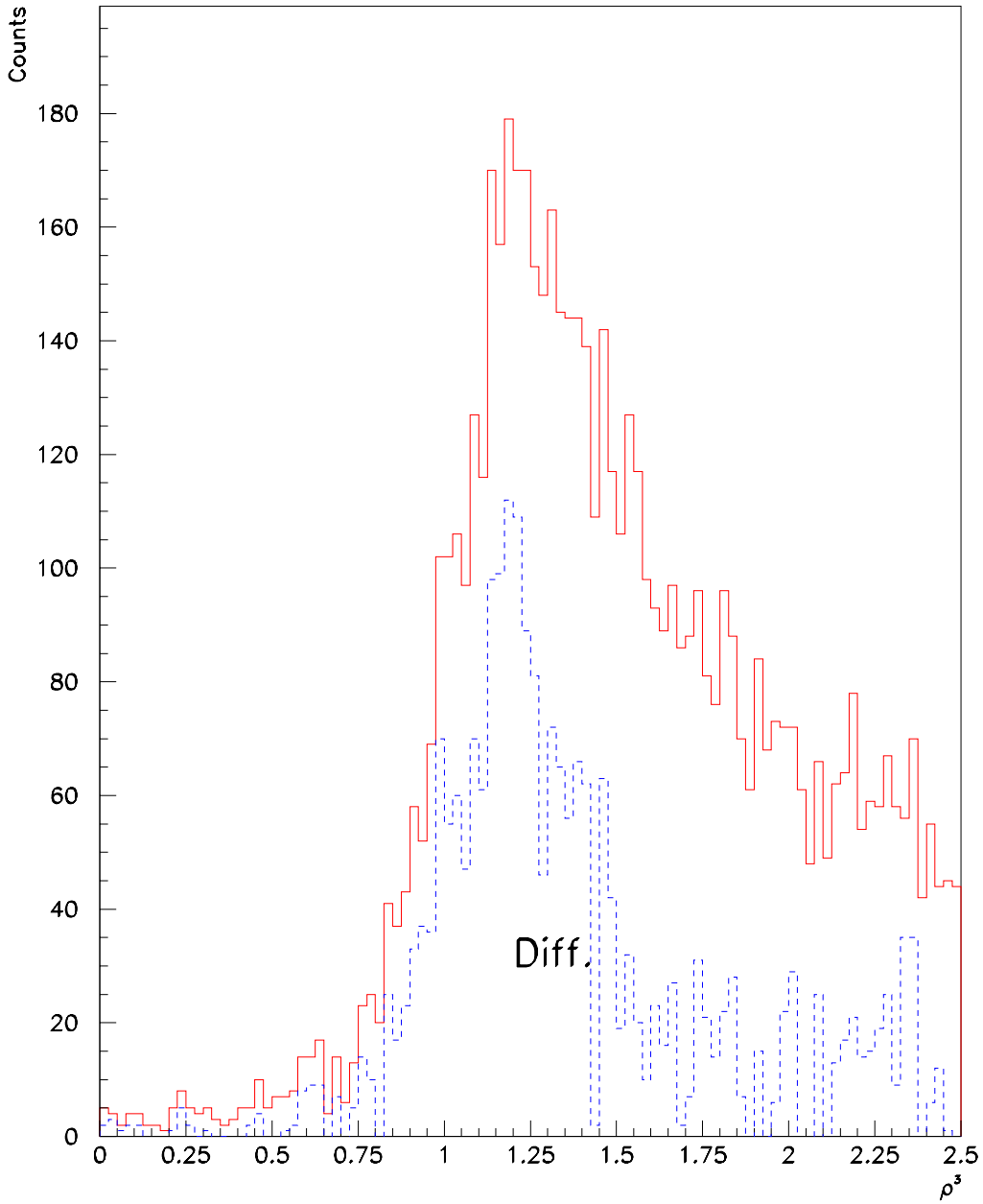

Figure 12: The R^3_{fit} distributions of those events in the cluster cut window are compared to those in a random cut window of the same size in the ($\cos\theta$,ϕ) space. The solid histogram is the R^3_{fit} distribution of the events in the cluster cut window. And the dashed histogram is the difference between this last distribution and that for a random cut window. In this plot, the plotted quantity ρ^3 is equivalent to $(R_{fit}/600\text{cm})^3$.

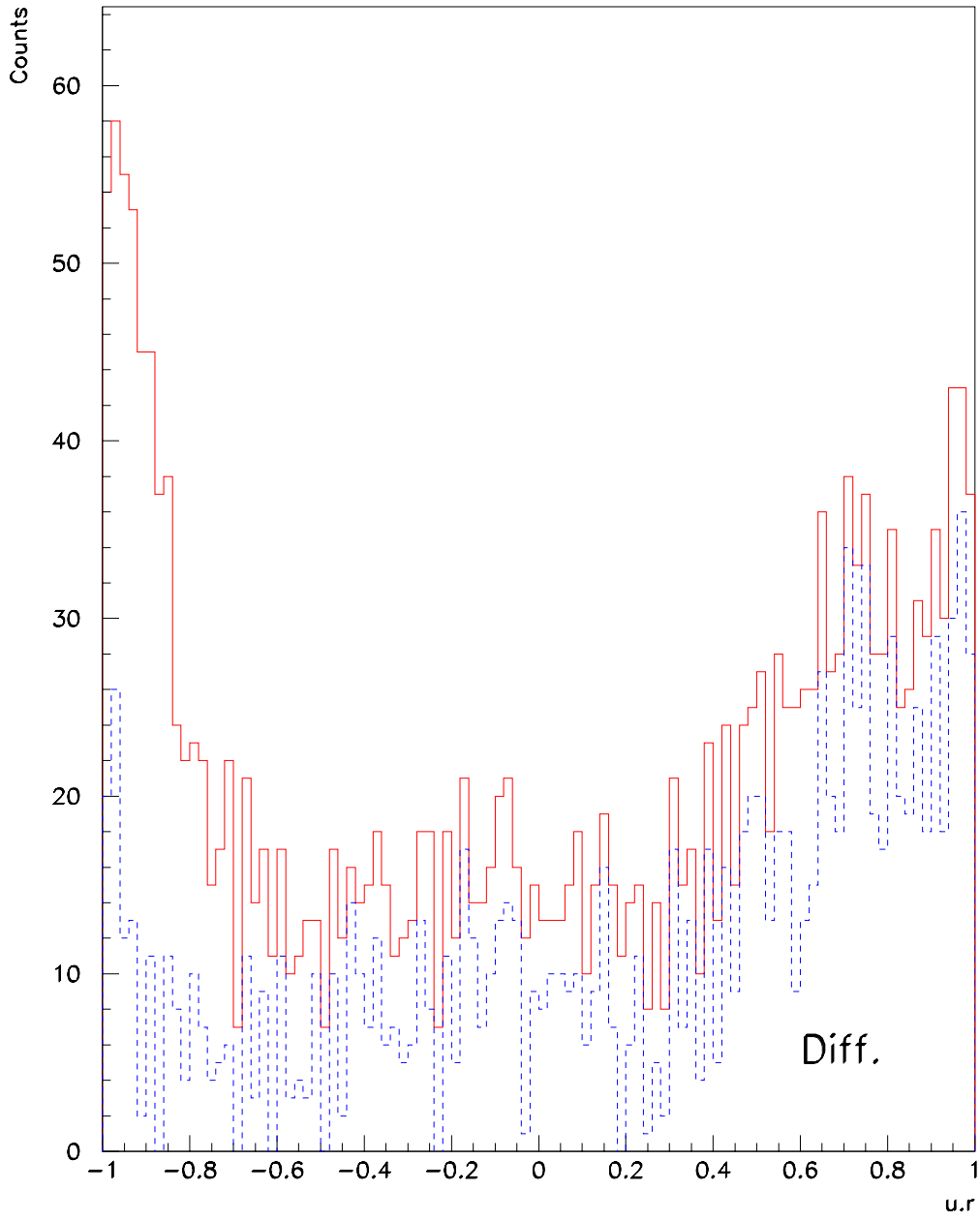

Figure 13: The $u \cdot r$ distributions of those events in the cluster cut window are compared to those in a random cut window of the same size in the ($\cos\theta$,ϕ) space. The solid histogram is the $u \cdot r$ distribution of the events in the cluster cut window. And the dashed histogram is the difference between this last distribution and that for a random cut window.

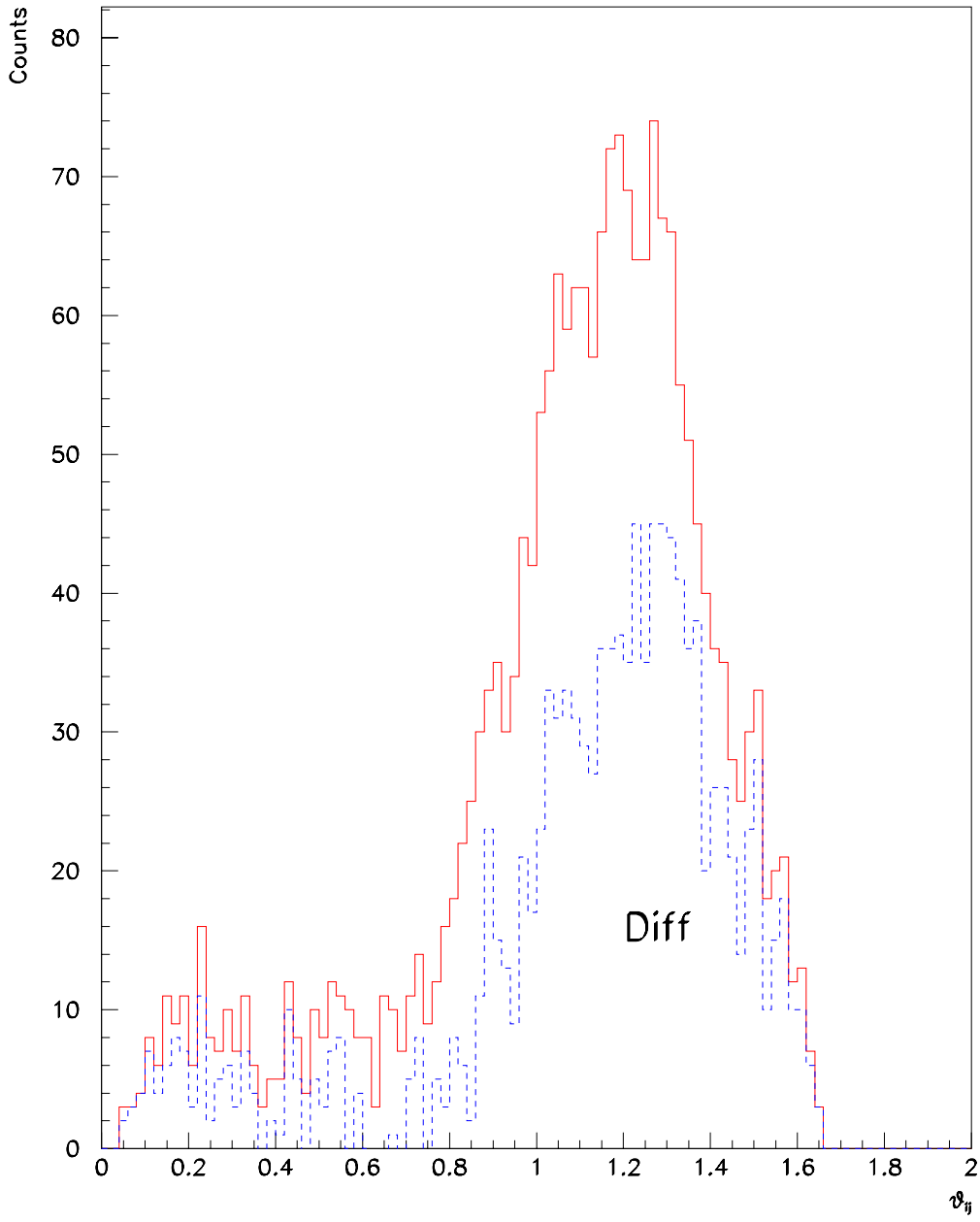

Figure 14: The θ_{ij} distributions of those events in the cluster cut window are compared to those in a random cut window of the same size in the ($\cos\theta$,ϕ) space. The solid histogram is the θ_{ij} distribution of the events in the cluster cut window. And the dashed histogram is the difference between this last distribution and that for a random cut window.

3 Summary

There is no evidence for any dependence of the event rate in the FiST or DAMN reduced data sets on the state of D_2O circulation. However, we found a cluster of events that are reconstructed close to the major repair done on the acrylic events. The Nhits distribution for this cluster is consistent with that of U and Th $\beta - \gamma$ events. We are investigating the origin of this clustering.

References

[1] H. Lee, *private communication*, 2000.

[2] E.D. Earles, *private communication*, 2000.